

Soft-chemical derived $\text{Bi}_2\text{O}_3\text{--ZnO--Ta}_2\text{O}_5$ nanopowder and ceramics

S.M. Zanetti*, M.G.S. Pereira, M.C.A. Nono

Laboratório Associado de Sensores e Materiais, Instituto Nacional de Pesquisas Espaciais, Av. dos Astronautas, 1758, Jd. da Granja, 12227-010 S. J. dos Campos, SP, Brazil

Available online 21 March 2007

Abstract

In this paper, the synthesis of bismuth zinc tantalate pyrochlore ($\text{Bi}_{1.5}\text{ZnTa}_{1.5}\text{O}_7$, α -BZT) by a soft-chemical method, based on the polymeric precursors, was investigated in order to obtain chemically homogeneous powders. The pyrochlore phase was investigated by X-ray diffraction, UV–vis and Raman spectroscopy. The study of α -BZT formation reveals that, at 600 °C, a single-phased nanopowder was obtained without any detectable intermediary or secondary phases. The morphology of the powders was examined by scanning electron microscope; the mean size distribution was measured by low angle laser light scattering. Both measurements showed a nanoscaled powder with large soft agglomerated clusters. The optical gap, obtained from the UV–vis spectra, ranged from 2.5 to 3.2 eV for the powders treated from 500 to 900 °C, respectively. © 2007 Elsevier Ltd. All rights reserved.

Keywords: Powders-chemical preparation; $\text{Bi}_2\text{O}_3\text{--ZnO--Ta}_2\text{O}_5$; Pyrochlore; Microwave dielectrics

1. Introduction

In last years, pyrochlore compounds in the ternary system $\text{Bi}_2\text{O}_3\text{--ZnO--Me}_2\text{O}_5$ (Me = Nb and Ta) have been recognized as potential candidates for capacitor and high-frequency filter applications due to their low temperature sintering characteristics.^{1,2} One of the main applications of these compounds is for manufacturing low temperature-firing high-frequency multilayer capacitors with internal silver electrodes. With recent developments in microwave devices, the compatibility of sintering ceramic with metal electrodes has been emphasized. For better performance of the devices, the interaction between the metal electrode and the ceramic shall be minimized by using single-phase powders.

The system $\text{Bi}_2\text{O}_3\text{--ZnO--Nb}_2\text{O}_5$ (BZN) has been extensively studied,^{3–6} however, less attention has been paid to the system $\text{Bi}_2\text{O}_3\text{--ZnO--Ta}_2\text{O}_5$ (BZT). BZT-based dielectrics ceramics have been systematically prepared by the conventional powder processing method and their powders and ceramics studied.^{7–11} Youn et al.¹ reported the occurrence of recalcitrant secondary phases due to the preferential reaction between Bi_2O_3 and Ta_2O_5 in the conventional processing. It is known that the solid state reaction process can lead to some local chemical heterogeneity and large sized particles, yielding multiphase powders.¹²

Hence, chemical methods have been an alternative for achieving smaller sized particles with chemical homogeneity.¹³ It is expected to obtain chemically homogeneous and phase-pure specimens, a narrow size distribution of particles, and low crystallization and sintering temperatures of the materials when the solution-based chemical methods are employed to prepare nanocrystalline materials.

This work aimed principally to achieve chemically homogeneous cubic-BZT nanopowders. For that a soft-chemical route was employed via an aqueous polymeric precursor method. The aqueous polymeric precursor is a modified Pechini process¹⁴ which has been successfully used for the synthesis of several complex oxides.^{15–17}

2. Experimental procedure

The starting reagents were Bi_2O_3 (99.99%, Aldrich), $(\text{CH}_3\text{CO}_2)_2\text{Zn}\cdot 2\text{H}_2\text{O}$ (99.5%, Carlo Erba), and $\text{Ta}(\text{OH})_5\cdot n\text{H}_2\text{O}$ (99.5%, CIF, S. J. Del Rei-MG, Brazil). The first step involved dissolving tantalum hydroxide in an aqueous solution of oxalic acid (OA), $\text{C}_2\text{H}_2\text{O}_4$ (99%, Fisher), at 80 °C. The aqueous suspension of tantalum hydroxide and oxalic acid was heated at boiling until complete dissolution to form tantalum oxalate (molar ratio OA/Ta = 4). The Ta content was gravimetrically determined as Ta_2O_5 . To this solution H_2O_2 (30%, Merck) was added in a molar ratio $\text{H}_2\text{O}_2/\text{metal}$ (Ta + Zn + Bi) = 4, and the pH was adjusted to 6 with NH_4OH . After homogenization

* Corresponding author.

E-mail address: zanetti@las.inpe.br (S.M. Zanetti).

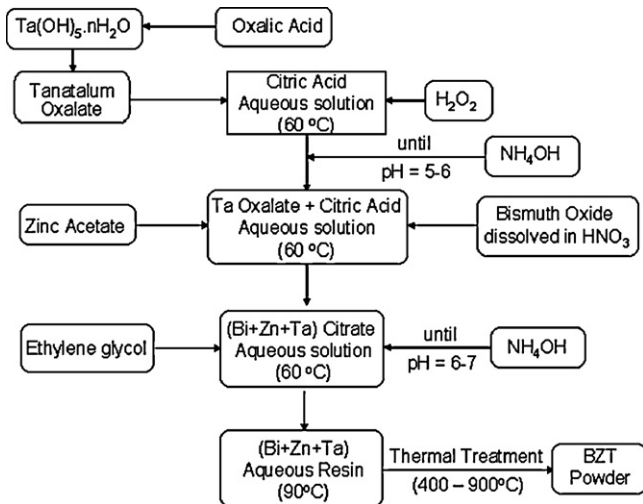


Fig. 1. Flowchart of BZT synthesis.

citric acid (CA), in a molar ratio $CA/metal = 3$, was added with constant stirring at $60\text{ }^{\circ}\text{C}$. Stoichiometric amounts of $(\text{CH}_3\text{CO}_2)_2\text{Zn}\cdot 2\text{H}_2\text{O}$ as salt and Bi_2O_3 , were added to the solution heated at $60\text{ }^{\circ}\text{C}$ to form a (Zn, Nb, Bi) complex precursor. The solution was kept under stirring at $60\text{ }^{\circ}\text{C}$ and the pH was adjusted to 6–7 with NH_4OH , resulting in a clear pale yellow solution. Ethylene glycol was added to this solution to promote polymerization of the mixed citrate. In this synthesis, the citric acid/ethylene glycol ratio (CA/EG, mass ratio) was 60/40. Fig. 1 shows the flowchart of the synthesis.

The resin was kept on a hot plate until a viscous gel was obtained, which was then thermally treated at $300\text{ }^{\circ}\text{C}$ for 4 h in a furnace. The powder thus obtained was treated at temperatures ranging from 500 to $900\text{ }^{\circ}\text{C}$ for 2 h to complete the crystallization process.

The crystalline phases were determined by X-ray powder diffraction (DRX) using a RIGAKU D/Max 2500 diffractometer, operating with the $\text{Cu K}\alpha$ radiation (40 kV, 150 mA). Raman spectra in the range of 300 – 1000 nm were obtained with a

RENISHAW U-3000 spectrometer furnished with a 632.8 nm He–Ne laser and coupled to an Olympus microscope, and the diffuse reflectance spectra (DRS) were recorded between 300 and 800 nm using a UV–vis–NIR spectrometer HITACHI, U3501.

The particle size distribution was determined by lower angle laser light scattering (LALLS) (MASTERSIZER 2000). In addition, a field emission scanning electron microscopy (FE-SEM) (JEOL 6400) was used to examine the morphology of the powders treated at different temperatures.

3. Results and discussion

The crystalline phase evolution for the α -BZT pyrochlore was followed by XRD, as shown in Fig. 2. At $500\text{ }^{\circ}\text{C}$ the powder was amorphous with some evidence of the pyrochlore phase nuclei. At $600\text{ }^{\circ}\text{C}$ the pyrochlore phase is already well crystallized although the peaks are some broad indicating small and disordered crystallites. As expected, the increase in the annealing temperature lead to higher crystallinity degree of the samples, as can be observed for powders treated at 700 , 800 and $900\text{ }^{\circ}\text{C}$. In this study, no detectable intermediary phases were observed at any time in the cubic-BZT composition, indicating that the chemical synthesis conferred a higher chemical homogeneity and reactivity on the powder. From the broadening of peaks of XRD patterns the crystallite sizes were calculate using the Scherrer equation. Crystallite size presented an exponential growth from 8 to 172 nm at 500 and $900\text{ }^{\circ}\text{C}$, respectively. The results are displayed in Fig. 2b.

Reports in literature¹⁷ state that the Raman spectrum of cubic BZT pyrochlore shows the following main bands: 182 , 267 , 445 , 545 and 761 cm^{-1} . Fig. 3 displays the Raman spectra of BZT powders treated at temperatures ranging from 500 to $900\text{ }^{\circ}\text{C}$. The broadness of the features, probably due to the nanometric particles, prevents an accurate estimation of the precise band frequencies. However, the Raman results allow confirming the powder single-phase nature observed by XRD even when treated at a low temperature ($600\text{ }^{\circ}\text{C}$). No extra bands were observed besides the band related to the cubic-BZT phase.

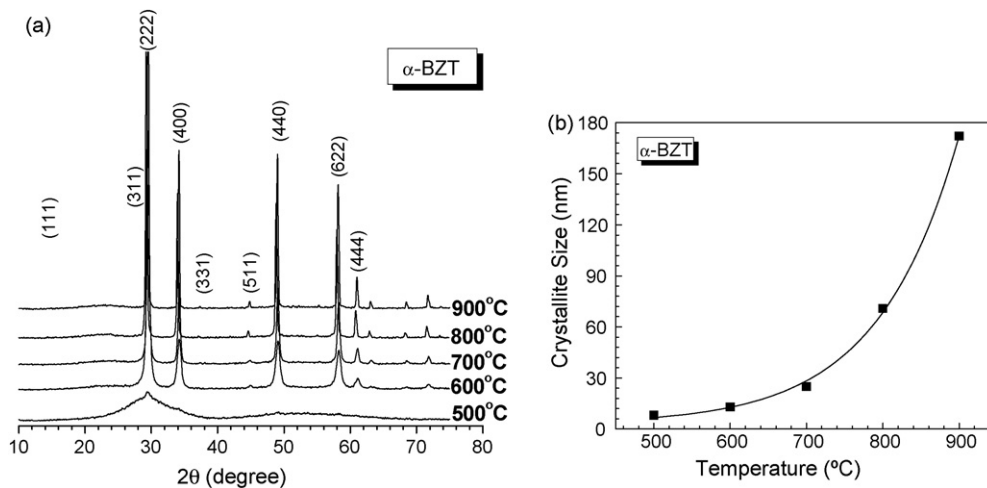


Fig. 2. (a) XRD patterns of BZT powders treated at different temperatures. (b) Crystallite size of BZT powders as a function of the temperature.

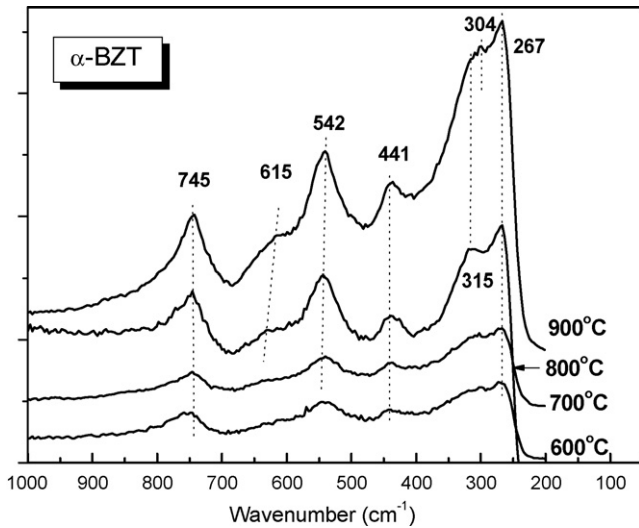


Fig. 3. Raman spectra of α -BZT powders treated at different temperatures for 2 h.

Fig. 4 shows the evolution of the diffuse reflectance spectra of BZT powders heat-treated at different temperatures. The absorbance values were calculated from the reflectance data, and the inset shows a plot of $(h\nu)^2$ against $h\nu$, from which the direct allowed band gap was estimated.¹⁸ The optical band gaps obtained from these spectra are displayed in Fig. 4b. At 500 °C, the band gap was 2.45 eV, indicating highly disordered phase, in accordance with the XRD data. At 600 °C, the band gap

increased to 3.38 eV. As the temperature increased, the band gap decreased to 3.26–3.19 eV in the powders treated from 700 to 900 °C, which is in agreement with the reported value (3.1 eV). The higher band gap value observed in the powder treated at 600 °C may be attributed to the crystallite size (15 nm).

The evolution of particle growth in the powders treated at different temperatures, was observed by SEM, the images clearly reveal the variation of the particle growth with thermal treatment (not shown). The powders treated from 500 to 700 °C are composed of large agglomerated clusters with dimensions of hundreds of nanometers. Annealing at 800 and 900 °C led to the formation of larger particles and homogeneous sintered clusters with grain sizes exceeding 1 μm , respectively. The powder treated at 700 °C was ball milled in isopropyl alcohol for 6 h in order to break big aggregates (Fig. 5a). The particle size distribution was measured by low angle laser light scattering in aqueous solution. A peak around 156 nm in diameter, which can be attributed to finer aggregates (XRD and SEM analysis showed crystallite and particle size around 30 nm) coexisting with reminiscent larger aggregates can be observed in Fig. 5b.

The maximum relative density of 87% was achieved for the pellet sintered at 1000 °C. The microstructure of the pellets, observed by SEM, showed a quite porous structure formed also by closed pores, which can be attributed to a poor compaction of green bodies (around 44%). The low relative density of green occurred due to aggregates, which in their turn are generated by the nanocrystalline nature of the obtained powders.

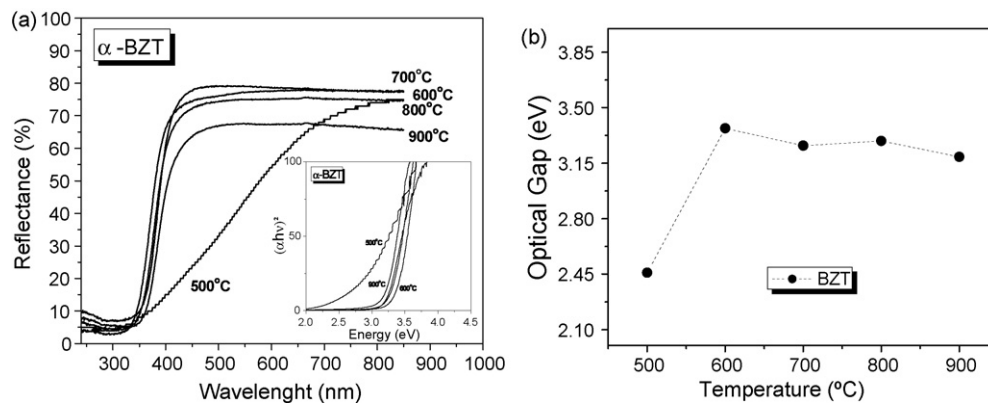


Fig. 4. (a) Diffuse reflectance of BZT powders treated at temperatures from 500 to 900 °C. (b) Optical gap as a function of the temperature.

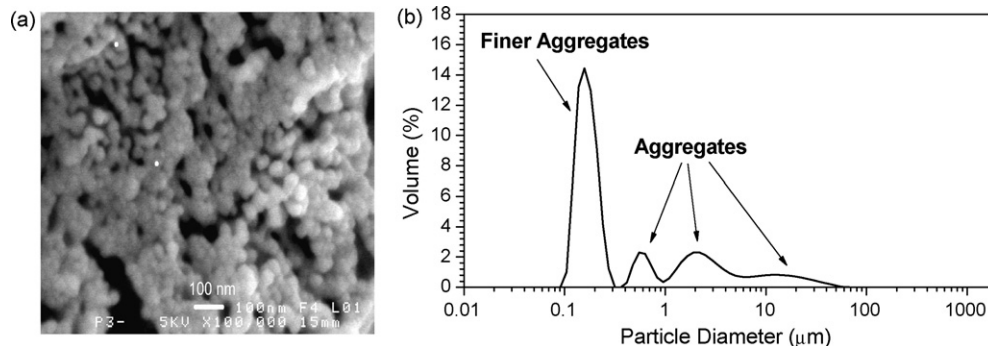


Fig. 5. BZT powder treated at 700 °C. (a) SEM image. (b) Particle size distribution measured by low angle laser light scattering.

4. Conclusion

$\text{Bi}_2\text{O}_3\text{-ZnO-Ta}_2\text{O}_5$ nanopowder was successfully synthesized by a soft-chemical route based on the polymeric precursor method. The study of phase formation revealed that a well-crystallized single-phased nanopowder was obtained after calcination at 600°C . The single-phase nature of the powder was confirmed by Raman spectra. The optical band gap for the powders treated between 600 and 900°C , calculated from diffuse reflectance spectra, was $3.4\text{--}3.2\text{ eV}$, indicating the low temperature crystallization of the pyrochlore phase. The low crystallization temperature and the phase purity of the nanopowder were attributed to the material's high chemical homogeneity and reactivity achieved by the chemical route.

Acknowledgements

The work was supported by the Brazilian financing agency FAPESP. The authors would like to thank LCSIM, Université de Rennes I, France, for the FE-SEM facilities, and LIEC, UFSCar, Brazil, for the XRD measurements.

References

1. Youn, H.-J., Sogabe, T., Randall, C. A., ShROUT, T. R. and Lanagan, M. T., Phase relations and dielectric properties in the $\text{Bi}_2\text{O}_3\text{-ZnO-Ta}_2\text{O}_5$ system. *J. Am. Ceram. Soc.*, 2001, **84**, 2557–2562.
2. Chen, A., Zhi, Y., Youn, H.-J., Randall, C. A., Bhalla, A. S., Cross, E. L. et al., Dielectric properties of $\text{Bi}_2\text{O}_3\text{-ZnO-Ta}_2\text{O}_5$ pyrochlore and zirconolite structure ceramics. *Appl. Phys. Lett.*, 2003, **82**, 3734–3736.
3. Nino, J. C., Lanagan, M. T. and Randall, C. A., Phase formation and reactions in the $\text{Bi}_2\text{O}_3\text{-ZnO-Nb}_2\text{O}_5\text{-Ag}$ pyrochlore system. *J. Mater. Res.*, 2001, **16**, 1460–1464.
4. Chen, S. Y., Lee, S. Y. and Lin, Y. J., Phase transformation, reaction kinetics and microwave characteristics of $\text{Bi}_2\text{O}_3\text{-ZnO-Nb}_2\text{O}_5$ ceramics. *J. Eur. Ceram. Soc.*, 2003, **23**, 873–881.
5. Wang, X. L., Wang, H. and Yao, X., Structures, phase transformations, and dielectric properties of pyrochlores containing bismuth. *J. Am. Ceram. Soc.*, 1997, **80**, 2745–2748.
6. Wang, H., Du, H. and Yao, X., Structural study of $\text{Bi}_2\text{O}_3\text{-ZnO-Nb}_2\text{O}_5$ -based pyrochlores. *Mater. Sci. Eng. B*, 2003, **99**, 20–24.
7. Youn, H.-J., Randall, C. A., Chen, A., ShROUT, T. R. and Lanagan, M. T., Dielectric relaxation and microwave dielectric properties of $\text{Bi}_2\text{O}_3\text{-ZnO-Ta}_2\text{O}_5$ ceramics. *J. Mater. Res.*, 2002, **17**, 1502–1506.
8. Peng, D., Shen, B., Zhang, L. and Yao, X., Study on relationship between sintering atmosphere and dielectric properties for $\text{Bi}_2\text{O}_3\text{-ZnO-Ta}_2\text{O}_5$ system. *Ceram. Int.*, 2004, **30**, 1199–1202.
9. Shen, B., Zhai, J. and Yao, X., Dielectric relaxation and tunability of $\text{Bi}_2\text{O}_3\text{-ZnO-CaO-Ta}_2\text{O}_5$ ceramics. *Appl. Phys. Lett.*, 2005, **86**, 072902-1–072902-3.
10. Shen, B., Yao, X., Peng, D. and Kang, L., Structure and dielectric properties of $\text{Bi}_2\text{O}_3\text{-ZnO-CaO-Ta}_2\text{O}_5$ ceramics. *Ceram. Int.*, 2004, **30**, 1207–1210.
11. Shen, B., Yao, X., Kang, L. and Peng, D., Effect of CuO or/and V_2O_5 oxide additives on $\text{Bi}_2\text{O}_3\text{-ZnO-Ta}_2\text{O}_5$ -based ceramics. *Ceram. Int.*, 2004, **30**, 1203–1206.
12. Haijun, Z., Xiaolin, J., Yongjie, Y., Zhanjie, L., Daoyuan, Y. and Zhenzhe, L., The effect of the concentration of citric acid and pH values on the preparation of MgAl_2O_4 ultrafine powder by citrate sol-gel process. *Mater. Res. Bull.*, 2004, **39**, 839–850.
13. Paris, E. C., Leite, E. R., Longo, E. and Varela, J. A., Synthesis of PbTiO_3 by use of polymeric precursors. *Mater. Lett.*, 1998, **37**, 1–5.
14. Pechini, M., Method of preparing lead and alkaline earth titanates and niobates and coating methods to form the capacitor. US Patent 3,330,697, 1967.
15. Zanetti, S. M., Leite, E. R., Longo, E. and Varela, J. A., $\text{SrBi}_2\text{Nb}_2\text{O}_9$ thin films deposited by dip coating using aqueous solution. *J. Eur. Ceram. Soc.*, 1999, **19**, 1409–1412.
16. Zanetti, S. M., Leite, E. R., Longo, E., Araújo, E. B., Chiquito, A. J., Eiras, J. A. et al., An alternative chemical route for synthesis of $\text{SrBi}_2\text{Ta}_2\text{O}_9$ thin films. *J. Mater. Res.*, 2000, **15**, 2091–2095.
17. Du, H. and Yao, X., Structural trends and dielectric properties of Bi-based pyrochlores. *J. Mater. Sci. Mater. Electron.*, 2004, **15**, 613–616.
18. Weckhuysen, B. M. and Schoonheydt, R. A., Recent progress in diffuse reflectance spectroscopy of supported metal oxide catalysts. *Catal. Today*, 1999, **49**, 441–451.